

# Anti-proliferative and pro-apoptotic activity of GD2 ganglioside-specific monoclonal antibody 3F8 in human melanoma cells

Chun-Yen Tsao<sup>1,†</sup>, Francesco Sabbatino<sup>1,†</sup>, Nai-Kong V Cheung<sup>2</sup>, Jeff Chi-feng Hsu<sup>1,#</sup>, Vincenzo Villani<sup>1</sup>, Xinhui Wang<sup>1</sup>, and Soldano Ferrone<sup>1,\*</sup>

<sup>1</sup>Department of Surgery; Massachusetts General Hospital; Harvard Medical School; Boston, MA USA; <sup>2</sup>Department of Pediatrics; Memorial Sloan-Kettering Cancer Center; New York, NY USA

<sup>†</sup>These authors equally contributed to this work.

<sup>#</sup>Present affiliation: Laboratory of Cell and Developmental Biology; National Institute of Dental and Craniofacial Research; National Institutes of Health; Bethesda, MD USA

**Keywords:** antibody, apoptosis, GD2 ganglioside, internalization, melanoma

**Abbreviations:** ADCC, antibody dependent cell mediated cytotoxicity; AIF, apoptosis inducing factor; anti-id, anti-idiotypic; Apaf-1, apoptotic protease activating factor 1; CCK-8, cell counting kit-8; CDC, complement dependent cytotoxicity; Ctr, control; CSPG4, chondroitin sulfate proteoglycan 4; FCS, fetal calf serum; FITC, fluorescein isothiocyanate; G.M., geometric mean; h, hour; HRP, horseradish peroxidase; IAP, inhibitor of apoptosis proteins; JC-1, 5,5',6,6'-tetrachloro-1,1',3,3'-tetraethylbenzimidazolcarbocyanine iodide; mAb, monoclonal antibody; min, minute; NHL, non-Hodgkin's lymphoma; p, phospho; PI, propidium iodide; PFA, paraformaldehyde; RT, room temperature; scFv, single-chain variable fragments; SCLC, small cell lung carcinoma; SD, standard deviations; XIAP, X-linked inhibitor of apoptosis protein

The beneficial clinical effects of immunotherapy with GD2-specific monoclonal antibodies (mAbs) in melanoma and neuroblastoma patients have stimulated interest in characterizing the mechanisms underlying their antitumor effects. Previous studies have shown that GD2-specific mAbs mediate complement- and cell-dependent cytotoxicity and induce caspase-dependent apoptosis of tumor cells. In this study, we showed that GD2-specific mAb 3F8, which is undergoing clinical evaluation, inhibited the *in vitro* growth and induced apoptosis of melanoma cells. This effect was dose- and time-dependent, mediated by the interaction of mAb 3F8 combining site with GD2 ganglioside, associated with GD2 expression level on the cell surface, mAb internalization and increase of GD2 containing endosomes triggered by mAb 3F8. The induction of apoptosis by mAb 3F8 was mediated by caspase 3-, 7-, and 8-dependent pathways, downregulation of the anti-apoptotic molecules survivin and cytochrome c, and caspase 9 independent-AIF release from mitochondria. In addition, analyses of signaling pathway components demonstrated that mAb 3F8 strongly inhibited AKT and FAK activation and increased cleaved PARP expression. These results indicated that multiple mechanisms played a role in the antitumor activity of mAb 3F8 in melanoma cells. This information should provide a mechanistic basis for the optimization of the rational design of immunotherapeutic strategies in the mAb-based treatment of GD2 positive tumors.

## Introduction

The disialoganglioside GD2 has been used as a target for antibody-based immunotherapy because of its high level of expression on neuroectoderm-derived human cancers, such as neuroblastoma,<sup>1</sup> melanoma,<sup>2,3</sup> and small cell lung carcinoma (SCLC).<sup>4</sup> Phase I/II clinical trials with GD2-specific mAbs have been implemented in both neuroblastoma<sup>5-9</sup> and melanoma,<sup>5</sup> and promising antitumor effects have been reported in patients with advanced neuroblastoma.<sup>5-7</sup> These encouraging clinical results have stimulated interest in defining the mechanisms

underlying the antitumor effects of GD2-specific mAb. GD2-specific mAbs mediate cell (ADCC)- and complement (CDC)-dependent cytotoxicity of cultured human melanoma cells.<sup>10-13</sup> GD2-specific mAbs have been also shown to directly inhibit the growth and induce apoptosis of GD2(+) human SCLC cells.<sup>4,14,15</sup> These effects are associated with activation and inhibition of caspase-dependent and MAPK pathway, respectively.<sup>4,15</sup> In contrast, limited information is available about the direct effects of GD2-specific mAb on melanoma cells and the underlying mechanisms. These topics are the subjects of the present manuscript.

\*Correspondence to: Soldano Ferrone; Email: sferrone@partners.org  
Submitted: 02/03/2015; Revised: 02/20/2015; Accepted: 02/20/2015  
<http://dx.doi.org/10.1080/2162402X.2015.1023975>

## Results

### Dose and time dependent inhibition by GD2-specific mAb of GD2(+) human melanoma cell growth

GD2-specific mAbs 3F8 and KM666 inhibited GD2(+) human melanoma HTB63 cell growth, while F(ab')<sub>2</sub> fragments of mAb 3F8 and GD2-specific mAb 5F11 and its single-chain variable fragments (scFv) fragments did not (data not shown). The anti-proliferative effects of mAb 3F8 were both dose- and time-dependent (Fig. 1A, B): growth inhibition was detectable at the concentration of 20 µg/ml and reached a maximum (~60%) at 100 µg/ml following a 72 h incubation (IC<sub>50</sub> = 50 µg/ml, Fig. 1A). The growth inhibition of HTB63 cells by mAb 3F8 was time-dependent, increasing from 30.1% following a 24 h incubation to 52.7% following a 72 h incubation (Fig. 1B). The growth inhibitory effect of mAb 3F8 was correlated with the level of GD2 expression ( $R^2 = 0.8132$  as determined by the two order polynomial regression, Fig. 1C). Three lines of evidence supported the GD2 specificity of this growth inhibitory effect of mAb 3F8. First, mAb 3F8 inhibited the growth of GD2(+) mouse melanoma cells B78-D14, but had no detectable effect on

the growth of the parental melanoma B16 cells, which do not express GD2 (data not shown). Second, the isotype matched mAb HO-1 had no detectable effect on cell growth (Fig. 1A, B). Lastly, inhibition by the anti-idiotypic (anti-id) mAb A1G4 of the binding of mAb 3F8 to GD2 on HTB63 cells inhibited its growth inhibitory effects (Fig. 1D).

### Induction of apoptosis by GD2-specific mAb 3F8 in GD2(+) human melanoma cells

GD2(+) HTB63 cells treated with mAb 3F8 showed a marked shrinkage of their cytoplasmic compartment (Fig. 1A). In contrast, no change of morphology was detected in cells incubated with the isotype matched mAb HO-1 (Fig. 1A). These changes in cell morphology were associated with a marked increase of percentage of apoptotic cells as detected by Annexin V/7-AAD staining (Fig. 2A) as well as by intracellular propidium iodide (PI) staining (Fig. 2B, upper panel). Following a 24 h incubation with mAb 3F8, 31%, and 20% of HTB63 cells were in apoptotic stage (Fig. 2A, B). The pro-apoptotic activity of mAb 3F8 was specific since incubation of HTB63 cells with the isotype matched mAb HO-1 induced apoptosis in only 7% and 2% of cells (Fig. 2A, B). The induction

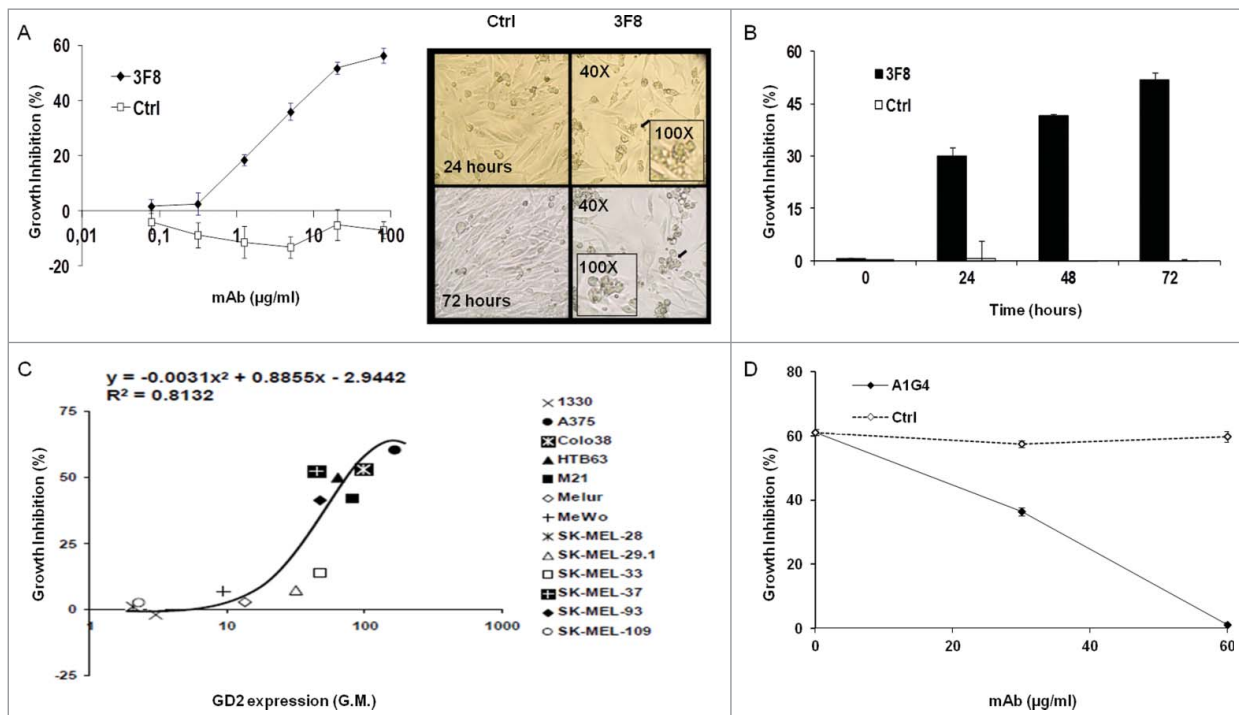


**Figure 1.** Inhibition by GD2-specific mAb 3F8 of GD2(+) human melanoma cell line growth. (A and B) HTB63 cells were seeded in flat bottom 96-well plates ( $3 \times 10^3$ /well) and incubated with the indicated concentrations of mAb 3F8. mAb HO-1 was used as an isotype matched control (Ctrl). Following an up to 72 h incubation at 37°C in a 5% CO<sub>2</sub> atmosphere, cell growth inhibition was determined by Cell Counting Kit-8 (CCK-8) assay (A) (left panel). Cell density and morphology of HTB63 cells were monitored under a bright field light microscope. Representative results of HTB63 cells treated with the mAb 3F8 or the isotype matched control mAb HO-1 (Ctrl) following an incubation at indicated times at 37°C in a 5% CO<sub>2</sub> atmosphere are shown. Magnification is indicated (A) (right panel). (C) Thirteen human melanoma cell lines were incubated with mAb 3F8 (20 µg/ml). Following an up to 72 h incubation at 37°C in a 5% CO<sub>2</sub> atmosphere, cell growth inhibition was determined by CCK-8 assay. Expression levels of GD2, defined as geometric mean (G.M.) fluorescence intensity of mAb 3F8 on the human melanoma cell lines tested (data not shown), was correlated with % of growth inhibition.  $R^2$  value as determined by the two order polynomial regression is indicated. The results presented are representative of those obtained in at least two independent experiments. (D) HTB63 cells were incubated with a mixture of mAb 3F8 (30 µg/ml) and anti-id mAb A1G4 (30 µg/ml). A mixture of mAb 3F8 and mAb MK2-23 (30 µg/ml) was used as a specificity control (Ctrl). Following an up to 48 h incubation at 37°C in a 5% CO<sub>2</sub> atmosphere, cell growth inhibition was determined by CCK-8 assay. Data are expressed as mean  $\pm$  standard deviations (SD) of the results obtained in three independent experiments.

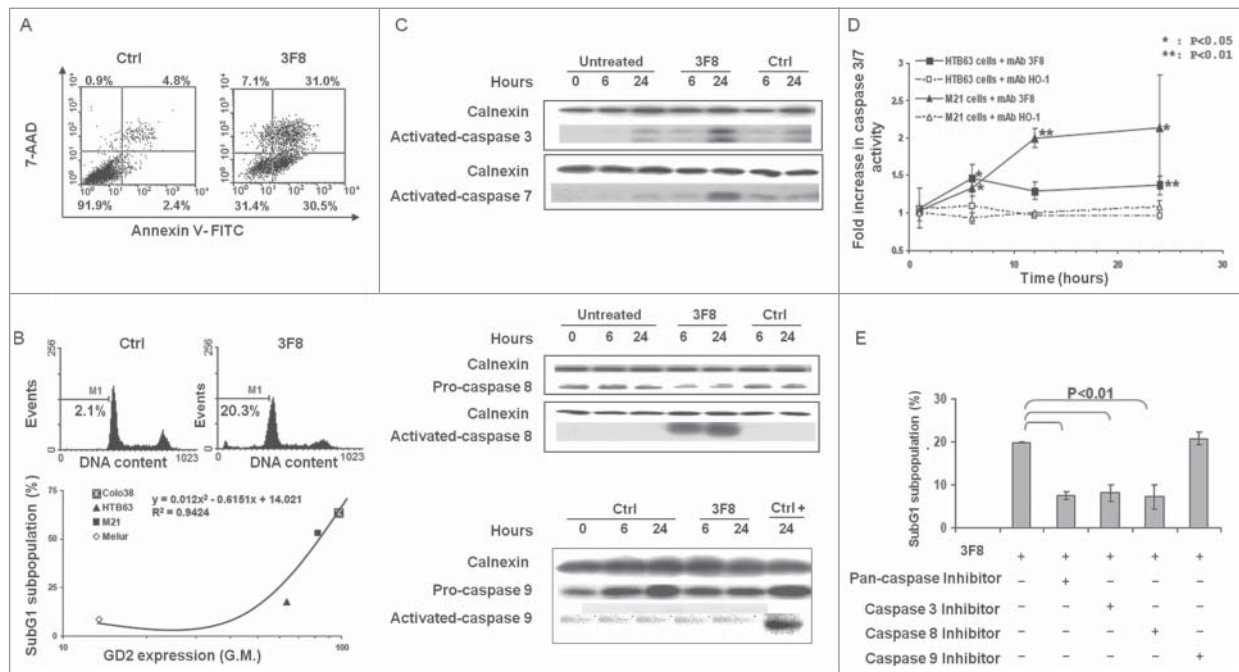


**Figure 2.** Apoptosis induction by GD2-specific mAb 3F8 in human melanoma cell lines. **(A)** HTB63 cells were seeded in flat bottom six-well plates ( $2 \times 10^5$ /well) and incubated with mAb 3F8 (50  $\mu\text{g/ml}$ ). mAb HO-1 was used as an isotype matched control (Ctrl). Following a 48 h incubation at  $37^\circ\text{C}$  in a 5%  $\text{CO}_2$  atmosphere, apoptosis induction was determined by Annexin V/7-AAD staining. Percentage of cells in different phases of apoptosis is indicated. **(B)** Colo38, HTB63, M21 and Melur cells were incubated with mAb 3F8 (50  $\mu\text{g/ml}$ ). mAb HO-1 was used as an isotype matched control (Ctrl). Following a 24 h incubation at  $37^\circ\text{C}$  in a 5%  $\text{CO}_2$  atmosphere, apoptosis induction was determined by PI staining. A representative result obtained in HTB63 cells is shown (upper panel). Percentage of apoptotic cells detected as sub-diploid cells (SubG1 population) was correlated with expression levels of GD2 in the cell lines tested (lower panel).  $R^2$  value as determined by the two order polynomial regression is indicated. The results presented are representative of those obtained in three independent experiments. **(C)** HTB63 cells were incubated with mAb 3F8 (50  $\mu\text{g/ml}$ ). mAb HO-1 was used as an isotype matched control (Ctrl). Untreated cells (Medium) and Jurkat cells treated with etoposide were used as a background and as a positive control for caspase 9 induction (Ctrl +), respectively. Following an incubation at  $37^\circ\text{C}$  in a 5%  $\text{CO}_2$  atmosphere for the indicated times, cells were harvested and lysed. Cell lysates were analyzed by protein gel blot with the indicated mAbs. Calnexin was used as a loading control. The data shown are representative of the results obtained in three independent experiments. **(D)** HTB63 and M21 cells were incubated with mAb 3F8 (3F8) (50  $\mu\text{g/ml}$ ). Following an up to 24 h incubation at  $37^\circ\text{C}$  in a 5%  $\text{CO}_2$  atmosphere enzymatic activity of activated caspase 3/7 in the cells was measured by Apo-ONE<sup>®</sup> Homogeneous Caspase 3/7 Assay. Data are expressed as mean  $\pm$  SD of the results obtained in three independent experiments. **(E)** HTB63 cells were pre-incubated with 40  $\mu\text{M}$  of the Pan-caspase inhibitor Boc-D-FMK, caspase 3 inhibitor Z-DQMD-FMK, caspase 8 inhibitor Z-IETD-FMK or caspase 9 inhibitor Z-LEHD-FMK. Following a 60 min incubation at  $37^\circ\text{C}$  in a 5%  $\text{CO}_2$  atmosphere cells were then incubated with mAb 3F8 (50  $\mu\text{g/ml}$ ). Following a 24 h incubation at  $37^\circ\text{C}$  in a 5%  $\text{CO}_2$  atmosphere apoptosis induction was determined by PI staining. Percentages of apoptotic cells detected as sub-diploid cells (SubG1 population) are shown. Data are expressed as mean  $\pm$  SD of the results obtained in three independent experiments.

of apoptosis in HTB63 cells by mAb 3F8 was also both time- and dose-dependent (Fig. S1) and influenced by the level of GD2 expression on human melanoma cells ( $R^2$  value = 0.9424) (Fig. 2B, lower panel).

#### Activation of caspase 3 and caspase 8 by GD2-specific mAb 3F8 in GD2(+) human melanoma cells

Treatment of both GD2(+) melanoma lines HTB63 and M21 with mAb 3F8 (50  $\mu\text{g/ml}$ ) activated caspase 3 and caspase 7 (Fig. 2C, D) as well as caspase 8 but did not activate caspase 9 (Fig. 2C). mAb 3F8-mediated apoptosis of HTB63 cells was >60% attenuated by pan-caspase inhibitors, Boc-D-FMK (40  $\mu\text{M}$ ) and Z-VAD-FMK (40  $\mu\text{M}$ ), by the caspase 3 inhibitor, Z-DQMD-FMK (40  $\mu\text{M}$ ) (Fig. 2E), and the caspase 8 inhibitor Z-IETD-FMK (Fig. 2E). In contrast, the caspase 9 inhibitor Z-LEHD-FMK (40  $\mu\text{M}$ ) had no detectable effect on apoptosis (Fig. 2E).

#### Release of cytochrome c and changes of mitochondria membrane permeability in HTB63 cells incubated with GD2-specific mAb 3F8

HTB63 cells showed an increase in mitochondria permeability (3.7 fold increase in the percentage of cells with high green fluorescence intensity) after incubation with mAb 3F8 (Fig. 3A). Moreover, the increase in mitochondria permeability of HTB63 cells incubated with mAb 3F8 was associated with the release into cytoplasm of both cytochrome c and apoptosis inducing factor (AIF) (Fig. 3B).

#### Downregulation of Apaf-1 and of the inhibitor of apoptosis protein survivin in HTB63 cells by GD2-specific mAb 3F8

Consistent with the lack of caspase 9 activation by mAb 3F8, the induction of apoptosis in HTB63 cells by mAb 3F8 was not suppressed by the caspase 9 inhibitor Z-LEHD-FMK (Fig. 2E). However, mAb 3F8 downregulated apoptotic protease activating

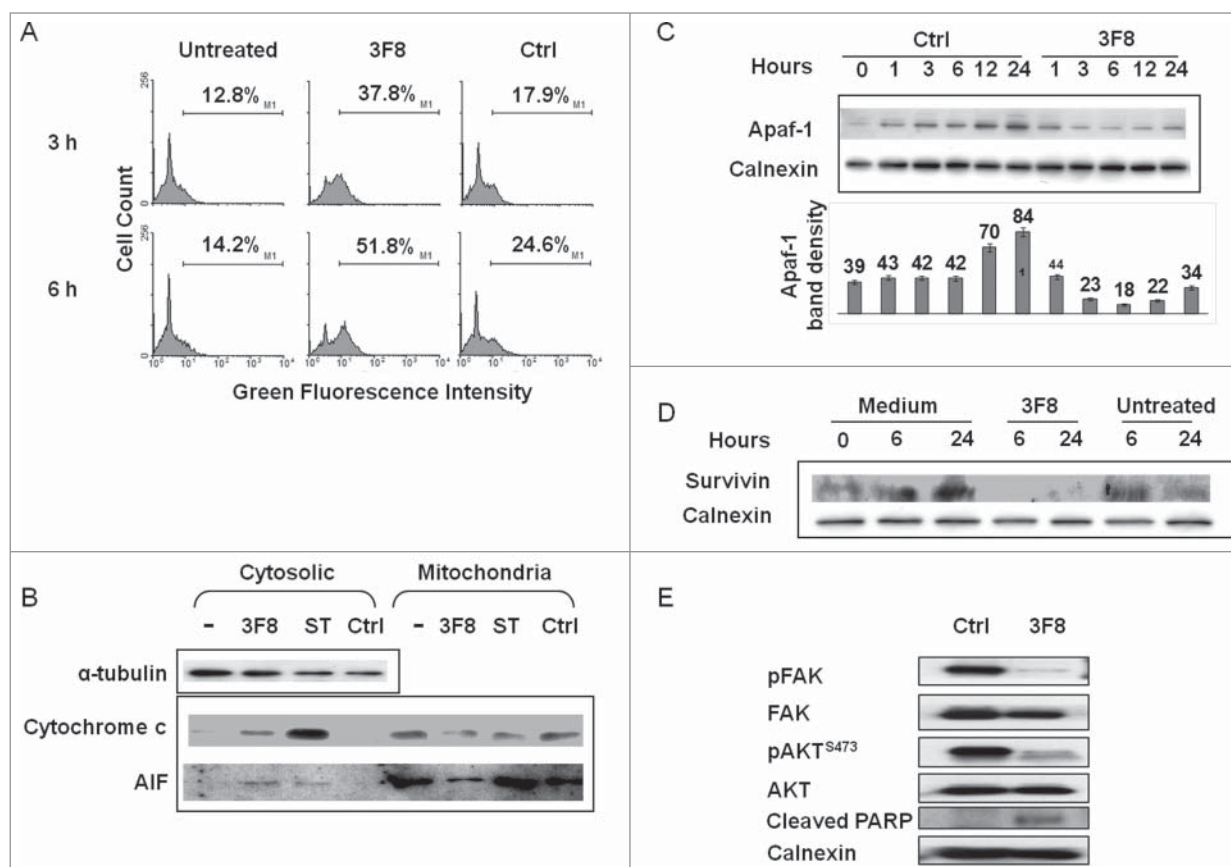


**Figure 3.** Changes in intrinsic caspase-dependent and caspase-independent apoptotic pathways induced by GD2-specific mAb 3F8 in human melanoma cells. **(A)** HTB63 cells were seeded in flat bottom six-well plates ( $2 \times 10^5$ /well) and incubated with mAb 3F8 (50  $\mu$ g/ml). mAb HO-1 was used as an isotype matched control (Ctrl). Untreated cells were used as a background control. Following an up to 6 h incubation at 37°C in a 5% CO<sub>2</sub> atmosphere, mitochondria permeability was determined by 5,5',6,6'-tetrachloro-1,1',3,3'-tetraethylbenzimidazolcarbocyanine iodide (JC-1) staining. Green fluorescence intensity of JC-1 in cells was measured by flow cytometry. Increase of green fluorescence intensity in cells represents increase in mitochondria permeability. The results presented are representative of those obtained in three independent experiments. **(B)** Following a 6 h incubation at 37°C in a 5% CO<sub>2</sub> atmosphere, cells were harvested and lysed. Cell lysates were analyzed by protein gel blot with the indicated mAbs. mAb HO-1 and staurosporine (0.5  $\mu$ M) were used as an isotype matched (Ctrl-) and as a positive (Ctrl+) control, respectively. Lysate from untreated cells was used as a background control (-).  $\alpha$ -tubulin was used as a loading control. The results presented are representative of those obtained in three independent experiments. **(C)** Following an up to 24 h incubation at 37°C in a 5% CO<sub>2</sub> atmosphere, cells were harvested and lysed. Cell lysates were analyzed by protein gel blot with the indicated mAbs. Calnexin was used as a loading control. A representative result is shown (upper panel). The levels of Apaf-1 normalized to calnexin are plotted and expressed as mean  $\pm$  SD of the results obtained in three independent experiments (lower panel). **(D)** Following an incubation at 37°C in a 5% CO<sub>2</sub> atmosphere for the indicated times, cells were harvested and lysed. Cell lysates were analyzed by protein gel blot with the indicated mAbs. Calnexin was used as a loading control. Lysate from untreated cells was used as a background control. The results presented are representative of those obtained in three independent experiments. **(E)** Following a 24 h incubation at 37°C in a 5% CO<sub>2</sub> atmosphere, cells were harvested and lysed. Cell lysates were analyzed by protein gel blot with the indicated mAbs. Calnexin was used as a loading control. The results presented are representative of those obtained in three independent experiments.

factor 1 (Apaf-1), a key component of caspase 9 activation (Fig. 3C). Apaf-1 protein in HTB63 cells incubated with mAb 3F8 for an up to 24 h at 37°C had a maximum three fold decrease as compared to its level in cells incubated with the isotype matched mAb HO-1 (Fig. 3C). Moreover, the level of survivin, an inhibitor of apoptosis proteins (IAP), was markedly reduced (Fig. 3D) in cells incubated with mAb 3F8, while that of X-linked inhibitor of apoptosis protein (XIAP), an inhibitor of apoptosis family of proteins IAP, displayed no detectable change (data not shown).

#### Modulation by GD2-specific mAb 3F8 of signaling pathway components in GD2(+) human melanoma cells

To investigate the potential causes of survivin and APAF-1 downregulation in GD2(+) melanoma cells, we investigated changes in the expression of signaling pathway components involved in the proliferation, survival, and apoptosis induction of melanoma cells. Incubation with mAb 3F8 markedly inhibited FAK and AKT activation, and enhanced cleaved PARP levels in HTB63 melanoma cells (Fig. 3E).



**Association of GD2-specific mAb 3F8 internalization and increase in GD2 containing endosomes with growth inhibition of HTB63 cells**

We then tested whether the internalization and clustering of mAb 3F8 could play a role in the apoptosis induction. Monitoring of mAb 3F8 trafficking showed the internalization of mAb 3F8 in HTB63 cells after less than 60 min (Fig. S2). mAb 3F8 internalized into HTB63 cells and co-localized with the endosomal marker Rab 5 (Figs. 4A and 5A). In addition, mAb 3F8 significantly ( $P < 0.05$ ) increased GD2-containing endosomes in HTB63 cells, compared to the irrelevant chondroitin sulfate proteoglycan 4 (CSPG4)-specific mAb 763.74, or to the F(ab')<sub>2</sub> fragments of mAb 3F8 (Figs. 4B, C and 5B, C). Lastly mAb 3F8 induced apoptosis and inhibited the growth of HTB63 cells while the irrelevant mAb 763.74 and F(ab')<sub>2</sub> fragments of mAb 3F8 had no detectable effects (Fig. 5D and data not shown).

**Discussion**

In agreement with the results available in literature using mAb 220–51<sup>4</sup> (mouse IgG3), mAb 9C4 (mouse IgG2a/IgG3)<sup>16</sup> and mAb ME361 (mouse IgG2a)<sup>17</sup> in SCLC, neuroblastoma and melanoma cells, we showed in this study that the GD2-specific mAb 3F8, a mouse IgG3 undergoing clinical evaluation, inhibits the growth and induces apoptosis of GD2(+) human and mouse melanoma cells. These data in conjunction with the growth inhibitory effects and induction of apoptosis by mAb 3F8 in human neuroblastoma and murine cell lines indicate that irrespective of tumor types, they can undergo cell death in the presence of GD2-specific mAb. However, this antitumor activity does not appear to be a general property of GD2-specific mAbs. According to Yoshida et al. mAb KM666 and KM1138 were less effective than mAb 220–51 in inhibiting growth of SCLC cells.<sup>4</sup> Furthermore, in our own experiments mAb KM666 was less

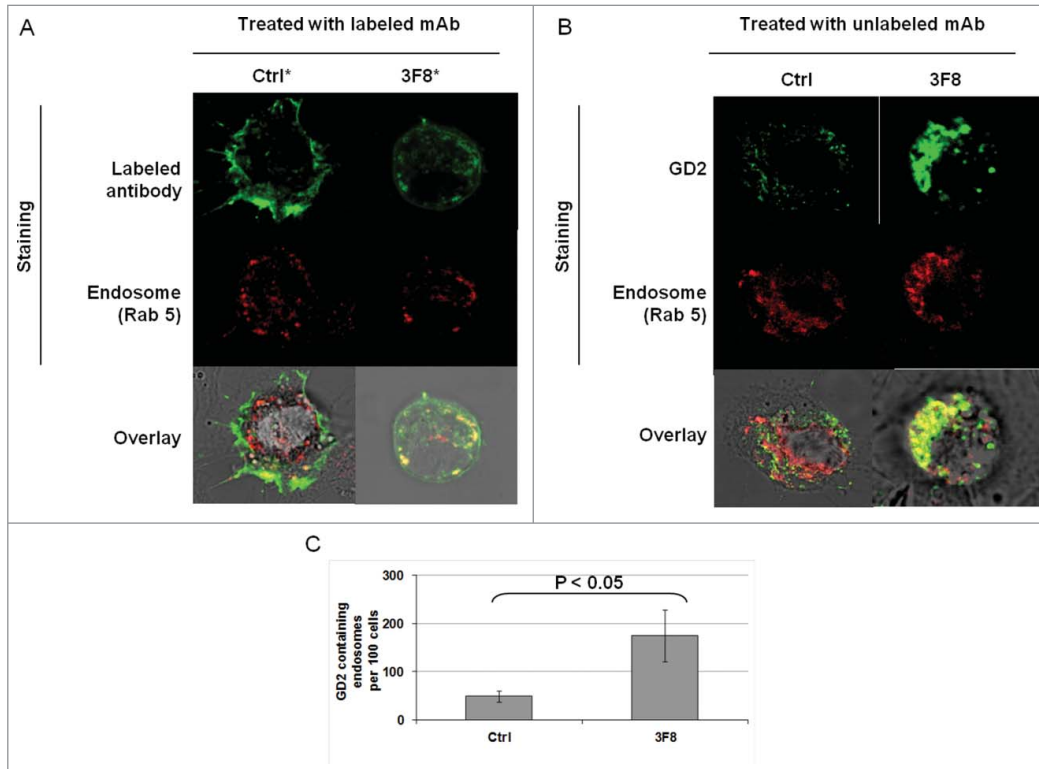


**Figure 4.** Internalization of GD2-specific mAb and increase of GD2 in endosomes in human melanoma cells incubated with GD2-specific mAb 3F8. (A) HTB63 cells ( $2 \times 10^5$ /well) were seeded and grown on glass coverslips in flat bottom six-well plates and incubated with Alexa Fluor 488 labeled mAb 3F8 (50  $\mu$ g/ml) (3F8\*). Alexa Fluor 488 labeled mAb 763.74 (50  $\mu$ g/ml) (Ctrl\*) was used as an irrelevant antibody control. Following a 3 h incubation at 37°C in a 5% CO<sub>2</sub> atmosphere, internalization of mAb 3F8 was determined by overlapping the confocal microscopy images of green fluorescence (Alexa Fluor 488 labeled mAb 3F8), and red fluorescence (endosomal marker, Rab 5). The results presented are representative of those obtained in two independent experiments. (B and C) HTB63 cells were incubated with mAb 3F8 (3F8) (50  $\mu$ g/ml). CSPG4-specific mAb 763.74 (50  $\mu$ g/ml) was used as a specificity control (Ctrl). Following a 3 h incubation at 37°C in a 5% CO<sub>2</sub> atmosphere, cells were harvested and intracellularly stained with Alexa Fluor 488 labeled GD2-specific mAb. Increase of GD2 containing endosomes (yellow color) in HTB63 cells was determined by overlapping the confocal microscopy images of green fluorescence (GD2-specific mAb) and red fluorescence (endosomal marker, Rab 5). The results presented are representative of those obtained in three independent experiments (B). Overlapped confocal microscopy images were analyzed by ImageJ software for the increase of GD2 containing endosomes (yellow particles). Data are expressed as mean of GD2 containing endosomes per 100 cells  $\pm$  SD of the results obtained in three independent experiments (C).

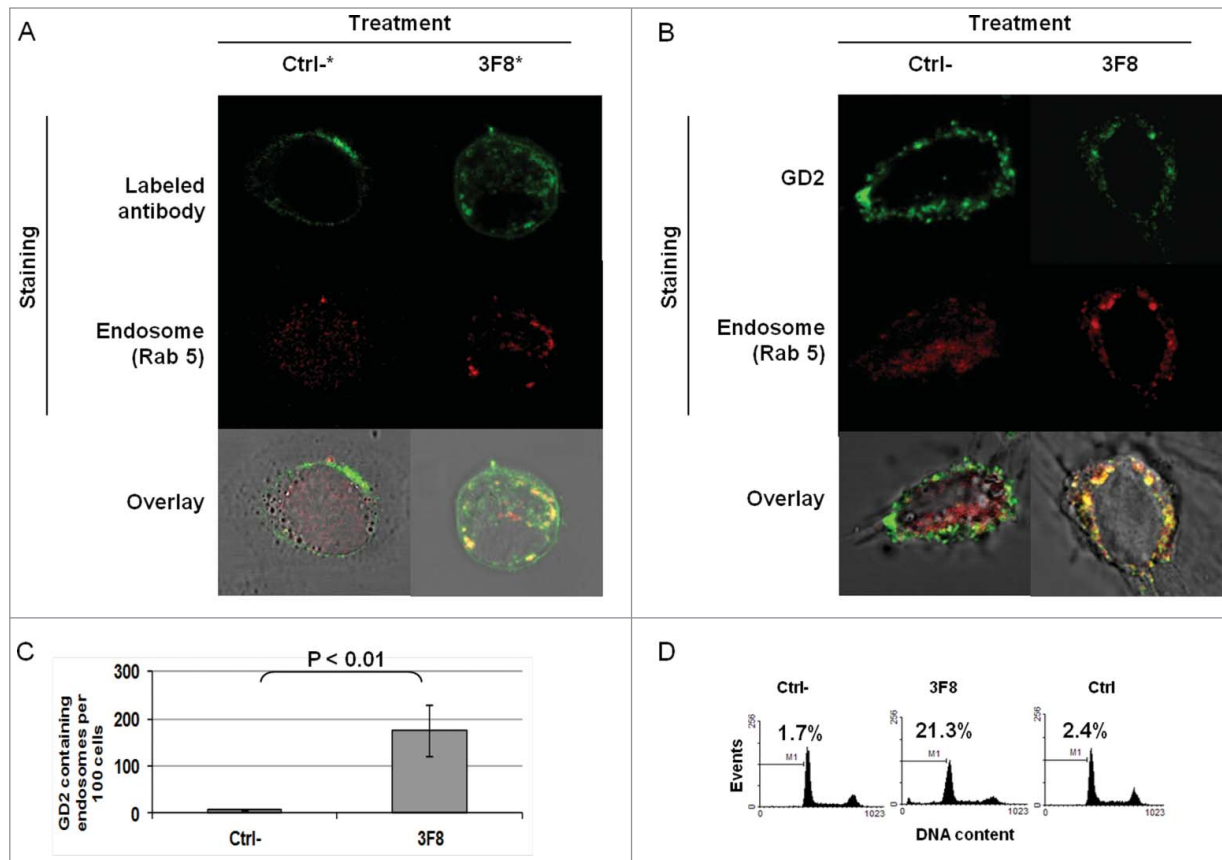


**Figure 5.** Association of apoptosis induction with GD2-specific mAb internalization and increase in GD2-containing endosomes in human melanoma cells incubated with GD2-specific mAb 3F8. **(A)** HTB63 cells ( $2 \times 10^5$ /well) were seeded and grown on glass cover slips in flat bottom six-well plates and incubated with Alexa Fluor 488 labeled GD2-specific mAb 3F8 (50  $\mu$ g/ml) (3F8\*). Alexa Fluor 488 labeled F(ab')<sub>2</sub> fragments of mAb 3F8 (50  $\mu$ g/ml) (Ctrl-\*) was used as a negative antibody control. Following a 3 h incubation at 37°C in a 5% CO<sub>2</sub> atmosphere, internalization of GD2-specific mAb 3F8 was determined by overlapping the confocal microscopy images of green fluorescence (GD2-specific mAb 3F8) and red fluorescence (endosomal marker, Rab 5). The results presented are representative of those obtained in three independent experiments. **(B and C)** HTB63 cells were incubated with mAb 3F8 (3F8) (50  $\mu$ g/ml). F(ab')<sub>2</sub> fragments of mAb 3F8 (50  $\mu$ g/ml) were used as a negative antibody control (Ctrl-). Following a 3 h incubation at 37°C in a 5% CO<sub>2</sub> atmosphere, cells were intracellularly stained with Alexa Fluor 488 labeled GD2-specific mAb. Increase of GD2 containing endosomes (yellow color) in HTB63 cells was determined by overlapping the confocal microscopy images of green fluorescence (GD2-specific mAb) and red fluorescence (endosomal marker, Rab 5) **(B)**. The results presented are representative of those obtained in three independent experiments. Overlapped confocal microscopy images were analyzed by ImageJ software for the increase of GD2 containing endosomes (yellow particles). Data are expressed as mean of GD2 containing endosomes per 100 cells  $\pm$  SD of the results obtained in three independent experiments **(C)**. **(D)** HTB63 cells were incubated with mAb 3F8 (50  $\mu$ g/ml). Following a 24 h incubation at 37°C in a 5% CO<sub>2</sub> atmosphere, induction of apoptosis was determined by intracellular PI-staining. F(ab')<sub>2</sub> fragments of mAb 3F8 were used as a negative antibody control (Ctrl-). mAb HO-1 was used as an isotype matched control (Ctrl-). The results presented are representative of those obtained in three independent experiments.

effective than mAb 3F8, while mAb 5F11 (an IgM), the scFv fragments of mAb 5F11, or the F(ab')<sub>2</sub> fragments of mAb 3F8 had no detectable effects on the growth of human melanoma cells. These results suggest that the Fc portion of mAbs (e.g., mouse IgG3) could play an important role in the anti-proliferative activity of GD2-specific mAbs with no relationship to the Fc-receptor. Instead, the differential ability of mAb 3F8 as compared with its F(ab')<sub>2</sub> fragments to inhibit cell growth and to induce apoptosis, could relate to the influence of its Fc fragment on internalization and the intracellular activation of apoptosis pathways. It is well-known that mouse IgG3 antibodies have a greater tendency to self-associate through the Fc than do antibodies derived from the other mouse IgG subclasses.<sup>18-22</sup> This could explain the loss of biologic effects of F(ab')<sub>2</sub> vs. intact mouse

IgG3 antibodies. When mouse 3F8 was humanized (mouse gamma 3 switched to human gamma 1), there was a 2–3 fold, but not substantial, decrease in affinity to GD2, commonly seen with CDR grafting.<sup>23</sup> In direct cytotoxicity assays of antibody induced cell death, IC<sub>50</sub> for mouse 3F8 was only 2–3 fold more potent than humanized 3F8.<sup>23</sup> While Fc-mediated cooperative binding could play some part in the biologic effect of mouse 3F8, it is probably a minor explanation for the anti-proliferative and pro-apoptotic activity of 3F8 in this manuscript.

For the first time, we have shown that the growth inhibition and the induction of apoptosis in melanoma cells by mAb 3F8 are both dose- and time-dependent, are influenced by the antigen density and require the interaction of the antigen combining site of mAb 3F8 with GD2 expressed on cell membrane. It is

noteworthy that the *in vitro* growth of six GD2(+) human melanoma cell lines, A375, Colo38, HTB63, M21, SK-MEL-37, and SK-MEL-93 was inhibited by antibody concentrations in the range of serum concentrations observed in patients with melanoma and neuroblastoma following the infusion of GD2-specific mAb.<sup>5,12,24</sup> Furthermore our results suggest that the administration of higher doses of GD2-specific mAb than those currently used may improve the clinical efficacy of this type of immunotherapy, since growth inhibition of HTB63 cells was maximal at the antibody concentration of 100 µg/ml and the peak serum concentration of GD2-specific mAb was in the range of 1.1–22.4 µg/ml in patients following mAb infusion (5–100 mg/m<sup>2</sup>/d).<sup>5,12,24</sup>

Although inhibition of cell growth could be secondary to induction of apoptosis or cell cycle arrest, the ratio of cells in G1/G0 phases and G2/M phases in the mAb treated cell population (examined by intracellular PI staining) was not significantly different from that in the control cell population. Similar to previous reports on apoptosis with GD2-specific mAbs,<sup>4,14,15,17</sup> the induction of apoptosis was caspase-dependent and correlated with the level of GD2 expression on melanoma cells. What was novel in our studies was the discovery of both extrinsic (caspase 8-dependent) and intrinsic (mitochondria-dependent) apoptotic pathways induced by mAb 3F8, although these pathways differed in the extent of their contribution. Specifically, the mAb 3F8 mediated-caspase-dependent apoptosis mainly involved the extrinsic apoptotic pathway, since changes of mitochondria permeability and release of cytochrome c by mAb 3F8 did not lead to the activation of caspase 9. On the other hand, caspase-independent apoptosis was demonstrated by the release of AIF, and the downregulation of Apaf-1 and survivin.<sup>25,26</sup> Downregulation of survivin has been associated with inhibition of the PI3K/AKT pathway in several solid tumors. The PI3K/AKT pathway plays a major role in survival and anti-apoptotic signal in melanoma. Our results are in line with this observation since induction of apoptosis and downregulation of anti-apoptotic proteins such as survivin are associated with inhibition of the AKT activation. Moreover, the ability of mAb 3F8 to trigger activation of caspase 8, release of cytochrome c and AIF, could be a mechanism for the induction of apoptosis by Apaf-1 downregulation, and in some neuroblastoma cells with caspase 8 gene silencing.<sup>27–30</sup>

In line with data by Yoshida et al. and by Aixinjueluo et al.,<sup>4,14,15</sup> we showed that GD2-specific mAb 3F8 inhibited FAK activation which has been associated with activation of p38 and induction of apoptosis. More importantly, we showed that the induction of apoptosis by mAb 3F8 was strongly associated with the internalization of mAb 3F8/GD2 and the increase of GD2 containing endosomes, which are not p38-dependent. These differences most likely reflect the different tumor origin of the cell lines tested, the surface density of the GD2, and/or the different binding kinetics of the mAb utilized.

Binding of an antibody to its target antigen on the cell surface has been shown to trigger sub-cellular signaling events through different mechanisms, such as antigen cross-linking and/or internalization of antibody-antigen complexes.<sup>31,32</sup> Internalization of ricin A-chain immunotoxin-conjugated GD2-specific mAb 14G2a (14G2a-RA) has also been described in 14G2a-RA

treated melanoma cells.<sup>31</sup> Besides the triggering of clustering and internalization of GD2 by mAb 3F8, we showed that induction of growth inhibition and apoptosis were strongly associated with the increase of GD2-containing endosomes in cells incubated with the GD2-specific mAb. This association and the translocation of cathepsin D into cytosol (data not shown) may account at least in part for the changes in mitochondria permeability induced by mAb 3F8, since an increase in endosomes of ceramide, a major GD2 component, leads to changes in mitochondria permeability.<sup>33</sup>

The apoptotic pathways utilized by mAb 3F8 were distinct from the already described p38-dependent apoptotic pathway utilized by GD2-specific mAb 220–51 in SCLC cells.<sup>15</sup> In addition, they were also different from the Src-dependent apoptotic pathways utilized by CD20 specific-rituximab in non-Hodgkin's lymphoma (NHL),<sup>34</sup> and from the p38- and JNK-dependent apoptotic pathways utilized by HER2-specific mAb in HER2 expressing tumor cells.<sup>35,36</sup>

In summary, our findings suggest that mAb 3F8 triggers apoptosis of GD2 expressing melanoma cells through multiple pathways (Fig. 6). These findings not only provide the underlying molecular mechanism for mAb 3F8 induced apoptosis in different tumor types, but also a useful framework to optimize immunotherapy with GD2-specific mAb.

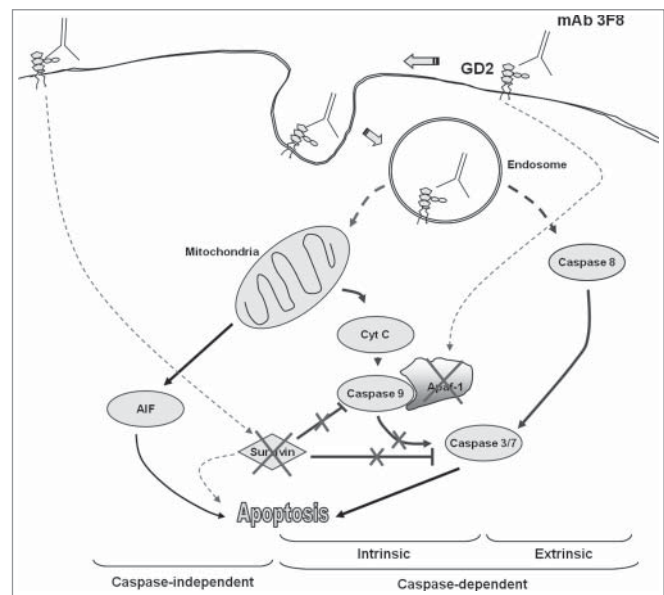


**Figure 6.** Proposed apoptotic pathways triggered by GD2-specific mAb 3F8. Following the internalization of both mAb 3F8 and GD2 into endosomes, the increase of GD2 containing endosomes triggers both extrinsic and intrinsic caspase-dependent and caspase-independent apoptotic pathways. They include the activation of caspase 3, 7, and 8, the release of cyt c and AIF, and the downregulation of both survivin and Apaf-1 without the activation of caspase 9. Apaf-1 downregulation is believed to be responsible for the lack of detectable caspase 9 activation. Survivin downregulation is believed to increase the sensitivity of cells to both caspase-dependent and caspase-independent apoptosis. Solid lines indicate the direct effects while dash lines indicate effects with either unknown or indirect mechanisms.

## Materials and Methods

### Cell lines and culture

Human melanoma cell lines 1330, A375, Colo38, HTB63, M21, Melur, MeWo, SK-MEL-28, SK-MEL-29.1, SK-MEL-33, SK-MEL-37, SK-MEL-93 and SK-MEL-109, and mouse melanoma cell lines B16 and B78-D14<sup>37</sup> were cultured in RPMI 1640 medium supplemented with 2 mmol/L L-glutamine (Mediatech, #10-043-CV) and 10% fetal calf serum (FCS; Atlanta Biologicals, #S11150) (complete medium). Cells were cultured at 37°C in a 5% CO<sub>2</sub> atmosphere.

### Reagents

Staurosporine (#02191400) was purchased from MP Biomedicals. Alexa Fluor 488 Protein Labeling Kit (#A10235) and Alexa Fluor 546 Monoclonal Labeling Kit (#A20183) were purchased from Molecular Probes. Pan-caspase inhibitors (Boc-D-FMK (#218745) and Z-VAD-FMK (#219007)) were purchased from Calbiochem. Caspase 3-, 8-, and 9-inhibitors (Z-DQMD-FMK (#2782-5), Z-IETD-FMK (#1148-5), and Z-LEHD-FMK (#1149-5)) were purchased from BioVision. CCK-8 (#CK04-05) was purchased from Dojindo Molecular Tech. Apo-ONE<sup>®</sup> Homogeneous Caspase 3/7 Assay (#G7790) was purchased from Promega.

### Antibodies

GD2-specific mAb 3F8 (IgG3),<sup>38</sup> F(ab')<sub>2</sub> fragments of mAb 3F8,<sup>11</sup> GD2-specific mAb 5F11 (IgM), scFv of mAb 5F11 (5F11scFv),<sup>39</sup> GD2-specific mAb 14G2a (IgG2a),<sup>40</sup> anti-id mAb A1G4 (recognizing an idiotope in mAb 3F8 antigen combining site),<sup>41</sup> mAb MK2-23 (IgG1) (recognizing an idiotope in the antigen combining site of the human CSPG4-specific mAb 763.74 (IgG1),<sup>42</sup> HLA-A2, A28-specific mAb HO-1 (IgG3) (unpublished results), and calnexin-specific mAb TO-5 (IgG1)<sup>43</sup> were prepared and characterized as described. GD2-specific mAb KM666 (IgG3)<sup>44,45</sup> was obtained from Kyowa Hakko Kogyo (Tokyo, Japan). All the antibodies are of mouse origin with the exception of mAb A1G4, which is of rat origin. Activated caspase 3- (#9661), 7- (#9491), 8- (#9496), 9- (#7237), total caspase 8- (#4790), total caspase 9- (#9502), phospho(p)-AKT- (#4060), AKT- (#4691), p-FAK- (#3283), FAK- (#3285), cleaved PARP- (#5625), survivin- (#2808) specific mAbs, Apaf-1- (#5088) and XIAP- (#2042) specific polyclonal antibodies were purchased from Cell Signaling Tech. Rab 5- (#sc-46692) specific mAb was purchased from Santa Cruz Biotechnology. Horseradish peroxidase (HRP)-conjugated goat anti-mouse IgG Fcy fragment (#115-036-071) and HRP-conjugated goat anti-rabbit IgG (H<sup>+</sup>L) (#111-035-144) antibodies were purchased from Jackson ImmunoResearch. Fluorescein isothiocyanate (FITC)-conjugated F(ab')<sub>2</sub> fragments of affinity-purified goat anti-mouse Ig antibody (#X092901) was purchased from DakoCytomation.

### Cell growth inhibition assay

Cell growth inhibition was determined by CCK-8 staining according to the manufacturer's instructions. All experiments were performed in triplicates. The growth inhibitory effects of

mAb 3F8 were calculated using the following formula: Growth Inhibition (%) = (1 - (O.D. 450 nm of mAb 3F8 treated well) / (O.D. 450 nm of non-treated well)) × 100.

### Determination of cell morphology

Cell morphology was examined by light microscopy (Axiovert 25, Carl Zeiss MicroImaging, Thornwood, NY). Images were acquired using Nikon Coolpix 4500 (Nikon, Melville, NY).

### Flow cytometry analysis

Cell surface staining was performed as described.<sup>46</sup> Apoptosis induction was detected by annexin V and 7-AAD kit (#559763) (BD Pharmingen<sup>™</sup>) cytometric staining according to the manufacturer's instructions. PI staining was performed as described.<sup>47</sup> The percentage of cells in the subG1 population as determined by subtracting the percentage of control cells from the percentage of treated cells in the subG1 population. Mitochondrial membrane potential was measured utilizing JC-1 (Molecular Probes, #T-3168) staining. Briefly, cells were seeded at the density of 1 × 10<sup>5</sup> per well in a six-well plate in complete medium and treated with the indicated doses of GD2-specific mAb 3F8 at 37°C in a 5% CO<sub>2</sub> atmosphere for the indicated times. The isotype matched mAb HO-1 was used as a control. JC-1 (10 μg/ml) was added to each well 30 min prior to the end of each incubation time. Cells were then harvested and resuspended in PBS at room temperature (RT). Data were acquired by FACScan flow cytometer (Becton-Dickinson Biosciences Immunocytometry Systems, San Jose, CA) and analyzed utilizing WinMDI software (The Scripps Research Institute, La Jolla, CA).

### Protein gel blot analysis

Protein gel blot assay for signaling pathway-related proteins was performed as described.<sup>48</sup>

### Measurement of caspase activity

The functional activity of caspase 3 was determined utilizing the Apo-ONE<sup>®</sup> Homogeneous Caspase 3/7 Assay following the manufacturer's protocol. Briefly, cells (2 × 10<sup>4</sup>/well) were incubated with mAb 3F8 (50 μg/ml) for up to 24 h at 37°C in a 5% CO<sub>2</sub> atmosphere in a black 384-well plate (384-well HTS plate, BrandTech, Essex, CT). Then cell suspension was incubated with 1:1 volume ratio of Apo-ONE<sup>®</sup> Caspase 3/7 reagent. Plates were then gently shaken at 500 rpm for 30 min and incubated for 1 h at RT. The fluorescence of each well was detected by the excitation wavelength of 490 nm and emission wavelength of 520 nm.

### Cytochrome c release assay

Cells were harvested, washed with ice-cold PBS, and fractionated by the ApoAlert Cell Fraction Kit (CLONTECH Laboratories, #630105). Lysates from cytosolic and mitochondrial fractions (20 μg protein per lane) were separated by 15% SDS-PAGE and then transferred onto an Immobilon-P transfer membrane. The membrane was analyzed by protein gel blot analysis with cytochrome c-specific antibodies (CLONTECH



Laboratories, #630105). Cell lysates incubated with 0.5  $\mu$ M staurosporine were used as a positive control.

### Immunostaining

HTB63 cells ( $2 \times 10^5$ /well) were seeded on glass cover slips in flat bottom six-well plates and incubated for 36 h at 37°C in a 5% CO<sub>2</sub> atmosphere. Cells were then incubated for up to 3 h at 37°C in a 5% CO<sub>2</sub> atmosphere with unlabeled mAb 3F8 or Alexa Fluor 488 (green) labeled mAb 3F8 (50  $\mu$ g/ml). Cells on coverslips were then washed twice with PBS and fixed with 2% paraformaldehyde (PFA) / PBS for 10 min at RT. Following three washings with PBS fixed cells were permeabilized with 0.2% Triton X-100/PBS for 5 min at RT. Permeabilized cells were then blocked with 1% BSA in PBS for 15 min at RT and stained overnight at 4°C with Alexa Fluor 546 (red) labeled Rab 5-specific antibody and/or Alexa Fluor 488 labeled GD2-specific mAb. Stained cells were mounted on a glass slide and examined under a fluorescence microscope or a confocal microscope. To maximize the staining of GD2 in cells, the Alexa Fluor 488 labeled GD2-specific mAb preparation contained both Alexa Fluor 488 labeled mAb 3F8 and Alexa Fluor 488 labeled mAb 14G2a (1:1 ratio). The co-localization of green and red fluorescence particles (yellow particles) (antibody or GD2 containing endosomes) in the confocal images was analyzed by ImageJ software (NIH, <http://rsb.info.nih.gov/ij/>).

### Antibody tracking in live cells

HTB63 cells ( $2 \times 10^5$ /well) were seeded on a glass bottom 24-well plate and incubated for up to 36 h at 37°C in a 5% CO<sub>2</sub> atmosphere. Seeded cells were then incubated with Alexa Fluor 488 labeled mAb 3F8 (50  $\mu$ g/ml) for up to 3 h at 37°C in a 5%

CO<sub>2</sub> atmosphere. The trafficking of Alexa Fluor 488 labeled mAb 3F8 on/in five selected HTB63 cells was monitored with an Axiovert 200M microscope (Carl Zeiss MicroImaging, Jena, Germany) with AxioVision software (Carl Zeiss MicroImaging) every 10 min for 3 h.

### Statistical analysis

The statistical significance of differences in the experimental results was analyzed utilizing the two-tailed, unpaired Student's *t*-test. Differences between groups were considered significant when the *p* value was < 0.05.

### Disclosure of Potential Conflicts of Interest

NKV Cheung was named as an inventor in a patent on humanized 3F8 filed by Memorial Sloan-Kettering Cancer Center.

### Funding

This work was supported by PHS grants RO1CA138188 and P50CA121973 awarded by the National Cancer Institute (SF), by Fondazione Umberto Veronesi Post-Doctoral Fellowship awarded by the Fondazione Umberto Veronesi (FS) and by Research Fellowship awarded by the Centro per la Comunicazione e la Ricerca del Collegio Ghislieri di Pavia (VV).

### Supplemental Material

Supplemental data for this article can be accessed on the publisher's website.

### References

- Schulz G, Cheresch DA, Varki NM, Yu A, Staffileno LK, Reisfeld RA. Detection of ganglioside GD2 in tumor tissues and sera of neuroblastoma patients. *Cancer Res* 1984; 44:5914-20; PMID:6498849
- Hershey P, Jamal O, Henderson C, Zardawi I, D'Alessandro G. Expression of the gangliosides GM3, GD3 and GD2 in tissue sections of normal skin, naevi, primary and metastatic melanoma. *Int J Cancer* 1988; 41:336-43; PMID:3346097; <http://dx.doi.org/10.1002/ijc.2910410303>
- Tsuchida T, Saxton RE, Morton DL, Irie RF. Gangliosides of human melanoma. *Cancer* 1989; 63:1166-74; PMID:2917320; [http://dx.doi.org/10.1002/1097-0142\(19890315\)63:6%3c1166::AID-CNCR2820630621%3e3.0.CO;2-5](http://dx.doi.org/10.1002/1097-0142(19890315)63:6%3c1166::AID-CNCR2820630621%3e3.0.CO;2-5)
- Yoshida S, Fukumoto S, Kawaguchi H, Sato S, Ueda R, Furukawa K. Ganglioside G(D2) in small cell lung cancer cell lines: enhancement of cell proliferation and mediation of apoptosis. *Cancer Res* 2001; 61:4244-52; PMID:11358851
- Cheung NK, Lazarus H, Miraldi FD, Abramowsky CR, Kallick S, Saarinen UM, Spitzer T, Strandjord SE, Coccia PF, Berger NA. Ganglioside GD2 specific monoclonal antibody 3F8: a phase I study in patients with neuroblastoma and malignant melanoma. *J Clin Oncol* 1987; 5:1430-40; PMID:3625258
- Cheung NK, Kushner BH, Cheung IY, Kramer K, Canete A, Gerald W, Bonilla MA, Finn R, Yeh SJ, Larson SM. Anti-G(D2) antibody treatment of minimal residual stage 4 neuroblastoma diagnosed at more than 1 year of age. *J Clin Oncol* 1998; 16:3053-60; PMID:9738575
- Cheung NK, Kushner BH, Yeh SD, Larson SM. 3F8 monoclonal antibody treatment of patients with stage 4 neuroblastoma: a phase II study. *Int J Oncol* 1998; 12:1299-306; PMID:9592190
- Cheung NK, Kushner BH, Kramer K. Monoclonal antibody-based therapy of neuroblastoma. *Hematol Oncol Clin North Am* 2001; 15:853-66; PMID:11765377; [http://dx.doi.org/10.1016/S0889-8588\(05\)70255-0](http://dx.doi.org/10.1016/S0889-8588(05)70255-0)
- Kushner BH, Kramer K, Cheung NK. Phase II trial of the anti-G(D2) monoclonal antibody 3F8 and granulocyte-macrophage colony-stimulating factor for neuroblastoma. *J Clin Oncol* 2001; 19:4189-94; PMID:11709561
- Munn DH, Cheung NK. Interleukin-2 enhancement of monoclonal antibody-mediated cellular cytotoxicity against human melanoma. *Cancer Res* 1987; 47:6600-5; PMID:3499978
- Cheung NK, Walter EI, Smith-Mensah WH, Ratnoff WD, Tykocinski ML, Medof ME. Decay-accelerating factor protects human tumor cells from complement-mediated cytotoxicity in vitro. *J Clin Invest* 1988; 81:1122-8; PMID:2450893; <http://dx.doi.org/10.1172/JCI113426>
- Kushner BH, Cheung NK. GM-CSF enhances 3F8 monoclonal antibody-dependent cellular cytotoxicity against human melanoma and neuroblastoma. *Blood* 1989; 73:1936-41; PMID:2653466
- Kushner BH, Cheung NK. Clinically effective monoclonal antibody 3F8 mediates nonoxidative lysis of human neuroectodermal tumor cells by polymorphonuclear leukocytes. *Cancer Res* 1991; 51:4865-70; PMID:1654202
- Yoshida S, Kawaguchi H, Sato S, Ueda R, Furukawa K. An anti-GD2 monoclonal antibody enhances apoptotic effects of anti-cancer drugs against small cell lung cancer cells via JNK (c-Jun terminal kinase) activation. *Jpn J Cancer Res* 2002; 93:816-24; PMID:12149148; <http://dx.doi.org/10.1111/j.1349-7006.2002.tb01324.x>
- Aixinjueluo W, Furukawa K, Zhang Q, Hamamura K, Tokuda N, Yoshida S, Ueda R, Furukawa K. Mechanisms for the apoptosis of small cell lung cancer cells induced by anti-GD2 monoclonal antibodies: Roles of anoikis. *J Biol Chem* 2005
- Lin CC, Shen YC, Chuang CK, Liao SK. Analysis of a murine anti-ganglioside GD2 monoclonal antibody expressing both IgG2a and IgG3 isotypes: monoclonality, apoptosis triggering, and activation of cellular cytotoxicity on human melanoma cells. *Adv Exp Med Biol* 2001; 491:419-29; PMID:14533812; [http://dx.doi.org/10.1007/978-1-4615-1267-7\\_27](http://dx.doi.org/10.1007/978-1-4615-1267-7_27)
- Doronin II, Vishnyakova PA, Kholodenko IV, Ponomarev ED, Ryazantsev DY, Molotkovskaya IM, Kholodenko RV. Ganglioside GD2 in reception and transduction of cell death signal in tumor cells. *BMC cancer* 2014; 14:295; PMID:24773917; <http://dx.doi.org/10.1186/1471-2407-14-295>
- Grey HM, Hirst JW, Cohn M. A new mouse immunoglobulin: IgG3. *J Exp Med* 1971; 133:289-304; PMID:5133863; <http://dx.doi.org/10.1084/jem.133.2.289>
- Abdelmoula M, Spertini F, Shibata T, Gyotoku Y, Luzuy S, Lambert PH, Izui S. IgG3 is the major source of cryoglobulins in mice. *J Immunol* 1989; 143:526-32; PMID:2738401

20. Garcia-Gonzalez M, Bettinger S, Ott S, Olivier P, Kadouche J, Pouletty P. Purification of murine IgG3 and IgM monoclonal antibodies by euglobulin precipitation. *J Immunol Methods* 1988; 111:17-23; PMID:3292650; [http://dx.doi.org/10.1016/0022-1759\(88\)90054-3](http://dx.doi.org/10.1016/0022-1759(88)90054-3)
21. Chapman PB, Yuasa H, Houghton AN. Homophilic binding of mouse monoclonal antibodies against GD3 ganglioside. *J Immunol* 1990; 145:891-8; PMID:1695649
22. Greenspan NS, Cooper LJ. Cooperative binding by mouse IgG3 antibodies: implications for functional affinity, effector function, and isotype restriction. *Springer Semin Immunopathol* 1993; 15:275-91
23. Cheung NK, Guo H, Hu J, Tassef DV, Cheung IY. Humanizing murine IgG3 anti-GD2 antibody m3F8 substantially improves antibody-dependent cell-mediated cytotoxicity while retaining targeting in vivo. *Oncol Immunology* 2012; 1:477-86; PMID:22754766; <http://dx.doi.org/10.4161/onci.19864>
24. Uttenreuther-Fischer MM, Huang C-S, Reisfeld RA, Yu AL. Pharmacokinetics of anti-ganglioside GD2 mAb 14G2a in a phase I trial in pediatric cancer patients. *Cancer Immunol, Immunother* 1995; 41:29-36; <http://dx.doi.org/10.1007/BF01788957>
25. Susin SA, Lorenzo HK, Zamzami N, Marzo I, Snow BE, Brothers GM, Mangion J, Jacotot E, Costantini P, Loeffler M et al. Molecular characterization of mitochondrial apoptosis-inducing factor. *Nature* 1999; 397:441-6; PMID:9989411; <http://dx.doi.org/10.1038/17135>
26. Li F, Ling X. Survivin study: an update of "What is the next wave?" *J Cell Physiol* 2006; 208:476-86; PMID:16557517; <http://dx.doi.org/10.1002/jcp.20634>
27. van Noesel MM, van Bezouw S, Voute PA, Herman JG, Pieters R, Versteeg R. Clustering of hypermethylated genes in neuroblastoma. *Genes Chromosomes Cancer* 2003; 38:226-33; PMID:14506696; <http://dx.doi.org/10.1002/gcc.10278>
28. Casciano I, Banelli B, Croce M, De Ambrosio A, di Vinci A, Gelvi I, Pagnan G, Brignole C, Allemanni G, Ferrini S et al. Caspase-8 gene expression in neuroblastoma. *Ann N Y Acad Sci* 2004; 1028:157-67; PMID:15650242; <http://dx.doi.org/10.1196/annals.1322.017>
29. Mustika R, Budiyo A, Nishigori C, Ichihashi M, Ueda M. Decreased expression of Apaf-1 with progression of melanoma. *Pigment Cell Res* 2005; 18:59-62; PMID:15649154; <http://dx.doi.org/10.1111/j.1600-0749.2004.00205.x>
30. Soengas MS, Gerald WL, Cordon-Cardo C, Lazebnik Y, Lowe SW. Apaf-1 expression in malignant melanoma. *Cell Death Differ* 2006; 13:352-3; PMID:16110320; <http://dx.doi.org/10.1038/sj.cdd.4401755>
31. Wargalla UC, Reisfeld RA. Rate of internalization of an immunotoxin correlates with cytotoxic activity against human tumor cells. *Proc Natl Acad Sci U S A* 1989; 86:5146-50; PMID:2544891; <http://dx.doi.org/10.1073/pnas.86.13.5146>
32. Iwabuchi K, Yamamura S, Prinetti A, Handa K, Hakomori S. GM3-enriched microdomain involved in cell adhesion and signal transduction through carbohydrate-carbohydrate interaction in mouse melanoma B16 cells. *J Biol Chem* 1998; 273:9130-8; PMID:9535903; <http://dx.doi.org/10.1074/jbc.273.15.9130>
33. Heinrich M, Neumeyer J, Jakob M, Hallas C, Tchikov V, Winoto-Morbach S, Wickel M, Schneider-Brachert W, Trauzold A, Hethke A et al. Cathepsin D links TNF-induced acid sphingomyelinase to Bid-mediated caspase-9 and -3 activation. *Cell Death Differ* 2004; 11:550-63; PMID:14739942; <http://dx.doi.org/10.1038/sj.cdd.4401382>
34. Jazirehi AR, Bonavida B. Cellular and molecular signal transduction pathways modulated by rituximab (rituxan, anti-CD20 mAb) in non-Hodgkin's lymphoma: implications in chemosensitization and therapeutic intervention. *Oncogene* 2005; 24:2121-43; PMID:15789036; <http://dx.doi.org/10.1038/sj.onc.1208349>
35. Hinoda Y, Sasaki S, Ishida T, Imai K. Monoclonal antibodies as effective therapeutic agents for solid tumors. *Cancer Sci* 2004; 95:621-5; PMID:15298722; <http://dx.doi.org/10.1111/j.1349-7006.2004.tb03319.x>
36. Nahta R, Esteva FJ. Herceptin: mechanisms of action and resistance. *Cancer Lett* 2006; 232:123-38; PMID:16458110; <http://dx.doi.org/10.1016/j.canlet.2005.01.041>
37. Becker JC, Varki N, Gillies SD, Furukawa K, Reisfeld RA. Long-lived and transferable tumor immunity in mice after targeted interleukin-2 therapy. *J Clin Invest* 1996; 98:2801-4; PMID:8981927; <http://dx.doi.org/10.1172/JCI119107>
38. Saito M, Yu RK, Cheung NK. Ganglioside GD2 specificity of monoclonal antibodies to human neuroblastoma cell. *Biochem Biophys Res Commun* 1985; 127:1-7; PMID:2579648; [http://dx.doi.org/10.1016/S0006-291X\(85\)80117-0](http://dx.doi.org/10.1016/S0006-291X(85)80117-0)
39. Cheung NK, Modak S, Lin Y, Guo H, Zanzonico P, Chung J, Zuo Y, Sanderson J, Wilbert S, Theodore LJ et al. Single-chain Fv-streptavidin substantially improved therapeutic index in multistep targeting directed at disialoganglioside GD2. *J Nucl Med* 2004; 45:867-77; PMID:15136638
40. Mujoo K, Kipps TJ, Yang HM, Cheresch DA, Wargalla U, Sander DJ, Reisfeld RA. Functional properties and effect on growth suppression of human neuroblastoma tumors by isotype switch variants of monoclonal anti-ganglioside GD2 antibody 14.18. *Cancer Res* 1989; 49:2857-61; PMID:2720646
41. Cheung NK, Canete A, Cheung IY, Ye JN, Liu C. Disialoganglioside GD2 anti-idiotypic monoclonal antibodies. *Int J Cancer* 1993; 54:499-505; PMID:8509225; <http://dx.doi.org/10.1002/ijc.2910540324>
42. Kusama M, Kageshita T, Chen ZJ, Ferrone S. Characterization of syngeneic anti-idiotypic monoclonal antibodies to murine anti-human high molecular weight melanoma-associated antigen monoclonal antibodies. *J Immunol* 1989; 143:3844-52
43. Ogino T, Wang X, Kato S, Miyokawa N, Harabuchi Y, Ferrone S. Endoplasmic reticulum chaperone-specific monoclonal antibodies for flow cytometry and immunohistochemical staining. *Tissue antigens* 2003; 62:385-93; PMID:14617045; <http://dx.doi.org/10.1034/j.1399-0039.2003.00114.x>
44. Ohta S, Honda A, Tokutake Y, Yoshida H, Hanai N. Antitumor effects of a novel monoclonal antibody with high binding affinity to ganglioside GD3. *Cancer Immunol Immunother* 1993; 36:260-6; PMID:8439988; <http://dx.doi.org/10.1007/BF01740908>
45. Ohta S, Igarashi S, Honda A, Sato S, Hanai N. Cytotoxicity of adriamycin-containing immunoliposomes targeted with anti-ganglioside monoclonal antibodies. *Anticancer Res* 1993; 13:331-6; PMID:8517645
46. Luo W, Hsu JC, Tsao CY, Ko E, Wang X, Ferrone S. Differential immunogenicity of two peptides isolated by high molecular weight-melanoma-associated antigen-specific monoclonal antibodies with different affinities. *J Immunol* 2005; 174:7104-10; <http://dx.doi.org/10.4049/jimmunol.174.11.7104>
47. Sabbatino F, Fuscillo C, Somma D, Pacelli R, Poudel R, Pepin D, Leonardi A, Carlomagno C, Della Vittoria Scarpati G, Ferrone S et al. Effect of p53 activity on the sensitivity of human glioblastoma cells to PARP-1 inhibitor in combination with topoisomerase I inhibitor or radiation. *Cytometry Part A: the journal of the International Society for Analytical Cytology* 2014; 85:953-61; PMID:25182801; <http://dx.doi.org/10.1002/cyto.a.22563>
48. Wang X, Osada T, Wang Y, Yu L, Sakakura K, Katayama A, McCarthy JB, Brufsky A, Chivukula M, Khoury T et al. CSPG4 protein as a new target for the antibody-based immunotherapy of triple-negative breast cancer. *J Natl Cancer Inst* 2010; 102:1496-512; PMID:20852124; <http://dx.doi.org/10.1093/jnci/djq343>